Acidity enhanced [Al]MCM-41 via ultrasonic irradiation for the Beckmann rearrangement of cyclohexanone oxime to ε-caprolactam

Zichun Wang[a], Huajuan Ling[a], Jeffrey Shi[a], Catherine Stampfl[b], Aibing Yu[c], Michael Hunger[d] and Jun Huang[a,*]

[a] Laboratory for Catalysis Engineering, School of Chemical and Biomolecular Engineering, The University of Sydney, NSW 2006, Australia

[b] School of Physics, The University of Sydney, Sydney, New South Wales 2006, Australia

[c] Department of Chemical Engineering, Monash University, Clayton, Victoria, 3800, Australia

[d] Institute of Chemical Technology, University of Stuttgart, D-70550 Stuttgart, Germany

[*] To whom correspondence should be addressed:

Tel: +61 2 9351 7483

Fax: +61 2 9351 2854

E-mail address: jun.huang@sydney.edu.au (Jun Huang)

Abstract

Using solid acid catalysts to replace liquid acids in the liquid-phase Beckmann rearrangement of cyclohexanone oxime (CHO) into ε-caprolactam (CPL) is crucial for the environmentally friendly production of synthetic fibers, such as Nylon-6. In this work, we prepared aluminum-containing MCM-41 catalysts under ultrasonic irradiation with various Si/Al ratios for this purpose. Quantitative ^{1}H MAS NMR investigations show that ultrasonic irradiation significantly promotes the formation of active Brønsted acid sites (BAS) on the [Al]MCM-41 catalysts up to 8 times higher than those prepared at the same conditions without ultrasonic irradiation, and up to 12 times higher BAS density than those reported in the literatures. The catalytic performance of [Al]MCM-41 catalysts can be strongly improved with increasing the BAS density, particularly to the ratio of BAS/(weakly acidic SiOH groups). Moreover, [Al]MCM-41 catalysts dehydrated at 393 K obtained two time higher CHO conversion and CPL yield than that dehydrated at 473 K. Hydrogen-bonded water molecules retained at low dehydration temperature may block surface SiOH groups and suppress the side reaction for cyclohexanone. With higher BAS density resulting from ultrasonic irradiation, [Al]MCM-41 catalyst (Si/Al = 10) in this work obtained the highest CPL yield among all [Al]MCM-41 materials reported for liquid-phase Beckmann rearrangement up to now. Finally, the reusability of [Al]MCM-41 catalyst was tested and no significant activity loss can be observed after five reaction cycles.

Keywords: MCM-41; room-temperature synthesis by ultrasonic irradiation; solid-state NMR; acid sites; Beckmann rearrangment.

1. Introduction

Beckmann rearrangement of cyclohexanone oxime (CHO) into ε-caprolactam (CPL), a key industrial intermediate of 4.5 million tons produced annually, is of great importance in the manufacturing of synthetic fibers and resins, such as Nylon-6 [1]. The production of CPL is currently dominated by concentrated sulfuric acid in large scale [2, 3]. To replace the harmful and corrosive liquid acids, recent works has focused on the development of environmentally friendly solid acids for the efficient production of CPL in a green chemical process.

A major industrial strategy is to develop solid acids for the liquid-phase Beckmann rearrangement [4-17]. It can produce CPL at moderate temperature (373-403 K) with less catalyst deactivation [8, 18], and the flexibility to replace homogeneous catalyst in existing plants, in comparison to that in the vapor-phase [19-24]. Crystalline zeolites and mesoporous silica-alumina (e.g. [Al]MCM-41), providing Brønsted acid sites (BAS) with easily tunable properties, are the most popular solid acid catalysts. Surface BAS are active sites to initialize the reaction via N-protonation to form an intermediate via a 1,2-H shift and dehydration, followed by rearrangement into the desired CPL [25], where higher BAS strength can promote the N-protonation [26]. However, the strong BAS on zeolites facilitate the formation of CPL at low temperature (< 373 K) but require high temperature for the desorption of CPL (523-623 K) from active sites [27], resulting in lower CPL selectivity and fast catalyst deactivation [10, 28]. Using a solvent (e.g. Bezonitrile (PhCN)) with suitable polarity and basicity can enhance the catalytic activity and prevent catalyst

deactivation [8, 11, 18]. Moreover, poisoning strong BAS and Lewis acid sites (LAS) via pre-adsorption of guest molecules (e.g. H_2O and PhCN) can significantly improve the catalytic performance of zeolite (e.g. HUSY) in the Beckmann rearrangement of CHO [9, 11].

Alternatively, [Al]MCM-41 materials possess BAS with relative weak acid strength compared to zeolite are favoured in Beckmann rearrangement reactions [8, 21-23]. It exhibits better catalytic performance than that of H-Beta zeolite with a CHO conversion of 50.6 % vs. 41 % and CPL selectivity of 89.1 % vs. 86.3 % [8]. Moreover, the catalytic performance of [Al]MCM-41 in the Beckmann rearrangement is significantly improved with decreasing Si/Al from 26.5 to 12 [8]. This is because BAS on [Al]MCM-41 are generated by Al species incorporated into the silica framework and flexibly coordinated to neighboring SiOH groups, where a higher Al content may promote the formation of BAS. It directs the current efforts to improve the catalytic performance of [Al]MCM-41 by introducing more Al species into the silica framework.

MCM-41 materials prepared by classic hydrothermal methods is often time and energy consuming (1-7 days at 333–423 K) [29-32]. Recently, the rapid room-temperature synthesis of MCM-41 has been introduced to prepare these materials in hours at milder conditions [25, 33-39]. Quantitative ^{1}H NMR spectroscopy shows the BAS density on [Al]MCM-41strongly increased from 0.013 to 0.121 mmol/g with decreasing Si/Al ratio from 50 to 15 [25]. These surface acidic OH groups are widely accepted to be generated by Al located in the vicinity of surface

SiOH groups, well known as tetrahedrally coordinated aluminum (Al^{IV}) species [25, 40, 41]. However, the conventional hydrothermal and sol-gel techniques with distinct inhomogeneity can result in Al species polymerized together (e.g. the different hydrolysis velocity of precursors) [42, 43], and lower the density of BAS on [Al]MCM-41.

It has been reported previously [44-47] that ultrasonic enhanced techniques can result in a sonochemical effects in liquid for continuous formation and growth of particles, implosive collapse of bubbles, and the sonochemical reactions at the interfacial region can introduce physicochemical change and enhance the liquid-solid mass transfer. These properties are able to homogeneously disperse silica oligomers in the mixture for efficient fabrication of [Si]MCM-41 in small particle size and a higher condensation degree [48]. In the preparation of MCM-41 with high titanium content, ultrasonic irradiation promotes the re-dispersion and condensation of inorganic species, resulting in titanium homogeneously distributed into the MCM-41 framework [49]. Similarly, the ultrasonic irradiation assisted sol-gel method is promising to improve the dispersion and condensation of Al into [Al]MCM-41 framework, and thus, promote the formation of BAS on the [Al]MCM-41 surface.

In this work, [Al]MCM-41 has been prepared at room temperature under ultrasonic irradiation. The mesoporous structure and texture of materials obtained have been studied by XRD and N_2 adsorption/desorption. The local structure and surface acid sites has been characterized by solid-state NMR spectroscopy. Quantitative ^1H MAS NMR spectroscopy shows [Al]MCM-41 prepared with

ultrasonic irradiation exhibit up to 8 times enhanced density of BAS. These [Al]MCM-41 materials were used as catalyst for the Beckmann rearrangement of CHO. A lower activation temperature was found to improve the catalytic performance of [Al]MCM-4. It is hypothesized that residual water molecules poison the strong sites on the surface.

2. Materials and Methods

2.1 Catalyst preparation

All chemicals used for the [Al]MCM-41 synthesis, such as an ammonium hydroxide solution (28 % NH_3 in H_2O), tetraethylorthosilicate (TEOS, > 98 %), hexadecyltrimethylammoniumchloride solution (CTACl, purum, ~ 25 % in H_2O), and aluminum sulfate octadecahydrate (> 98 %) were obtained from Sigma-Aldrich. The preparation method is similar to that described in our earlier work [25]. For a typical preparation of [Al]MCM-41, CTACl, an ammonium hydroxide solution, TEOS in a volume ratio of 1:1:1 in 500 ml demineralized water and a certain amount of aluminum sulfate octadecahydrate calculated based on Si/Al ratios were mixed under vigorous stirring at room temperature. Then the resulting mixture was immidiately subjected to sonication at room temperature for 1 h in an ultrasonic bath with a power of 300 W and ultrsonic frequency of 40 KHz. The resulting solid was filtered and washed with distilled water and then dried in an oven at 353 K. Finally, the obtained MCM-41 materials were calcined at 823 K with a heating rate of 1 K/ min in the presence of static air for 6 h. The nomenclature of [Al]MCM-41 is defined as

U-[Al]MCM-41/x, where U represents ultrasonic irradiation and x is the Si/Al ratios of 10, 20, 30, 40 and 50.

2.2 Characterization of textural and morphological properties

XRD characterization. Small-angle X-ray diffraction (XRD) studies were performed on a Siemens D5000 with Cu-Kα radiation in the range of 2-10°, and with scanning steps of 0.02°.

BET measurements. The surface area, average pore size, and total pore volume of the MCM-41 materials were determined by N_2 adsorption/desorption isotherms on an Autosorb IQ-C system. An amount of 50 mg of each sample was degassed at 423 K for 12 h under vacuum before the measurements and then recorded at 77 K.

2.3 Solid-state NMR investigation

Prior to ^{27}Al and ^{29}Si MAS NMR investigations, all samples were fully hydrated by exposure to the saturated vapor of $Ca(NO_3)_2$ solution at ambient temperature overnight in a desiccator. Before the ^{1}H and ^{13}C MAS NMR experiments, the samples were placed in glass tubes and dehydrated at 723 K for 12 h under a pressure of less than 10^{-2} bar. The dehydrated samples were sealed in the glass tubes or directly loaded with ammonia or acetone-2-^{13}C (99.5 % ^{13}C-enriched, Sigma-Aldrich) on a vacuum line. Subsequently, the loaded samples were evacuated at 393 K for 1 h (for ammonia) or at room temperature for 2 h (for acetone) to remove weakly physisorbed molecules. Subsequently, the samples were transferred into the MAS NMR rotors under dry nitrogen gas inside a glove box.

^{1}H, ^{27}Al, and ^{13}C MAS NMR investigations were carried out on a Bruker Avance III 400 WB spectrometer at resonance frequencies of 400.1, 104.3, and 100.6 MHz, respectively, and with the sample spinning rate of 8 kHz using 4 mm MAS rotors. The spectra were recorded after single-pulse π/2 and π/6 excitation with repetition times of 20 s and 0.5 s for studying ^{1}H and ^{27}Al nuclei, respectively. Quantitative ^{1}H MAS NMR measurements were performed using a zeolite H,Na-Y (35 % ion-exchanged) as an external intensity standard. ^{13}C cross-polarization (CP) MAS NMR spectra were recorded with a contact time of 4 ms and the repetition time of 4 s. The ^{29}Si MAS NMR spectra were performed on the same spectrometer using a 7 mm MAS NMR probe at the resonance frequency of 79.5 MHz and with the sample spinning rate of 4 kHz. Single-pulse π/2 excitation and high-power proton decoupling with a recycle delay of 20 s were applied.[50]

2.4 Catalytic reaction

The obtained U-[Al]MCM-41 catalysts were tested in the Beckmann arrangement of CHO to CPL. The reaction was carried out in a four-necked-round bottom flask equipped with a reflux condenser. Prior to reaction, the U-[Al]MCM-41 catalysts (50 mg) was pre-loaded in the flask and dehydrated in nitrogen gas flow (200 to 250 ml/min) at temperatures of 393 K or 473 K for 12 h in an oil bath. After cooling, a mixture of cyclohexane oxime (50 mg) and PhCN (10 ml) was injected into the flask and stirred during the reaction at 393 K for 7 h. The reaction products were analyzed using a gas chromatograph Shimadzu GCMS-QP2010 Ultra equipped with a Rtx-5MS capillary column (30 m × 0.25 mm × 0.25 μm) connected with a mass spectrometer

for qualitative analysis, and a RTX-5 capillary column (30 m × 0.32 mm × 3 μm) connected with a GC-FID detector for quantitative analysis. The selectivity to specific products i (S_i) was calculated by:

$$S_i\ (\%) = 100 \times (i) / [(CHO)_0\text{-}(CHO)] \quad (1)$$

where (i) is the molar concentration of the product i and $(CHO)_0$ and (CHO) correspond to the molar concentrations of PG before and after reaction, respectively.

3. Results and Discussion

3.1 Characterization of textural and morphological properties

The hexagonal framework of synthesized U-[Al]MCM-41 materials were confirmed by XRD patterns recorded in the small angle region (2θ = 2° - 10°) (Fig. 1) with a strong (100) reflection at low angles [25, 50]. In comparison with typical [Si]MCM-41 [25, 50], the (110) and (200) reflections at 4.3° and 4.9° became weak and broad, as well as the (100) reflections. This indicates the long range order of MCM-41 materials was strongly disturbed due to Al incorporated into the silica framework, typically observed with [Al]MCM-41 materials [25, 51, 52].

Figure 1.

The nitrogen adsorption/desorption isotherms and the corresponding BJH pore size distribution curves of U-[Al]MCM-41 samples are depicted in Fig. 2. All samples show type IV isotherms, corresponding to the mesoporous structure according to the IUPAC classification [53]. The pore size distributions are narrow and uniform for

mesoporous U-[Al]MCM-41 materials (insets in Fig. 2). The results of nitrogen adsorption were summarized in Table 1. The higher surface areas were obtained with all samples (887.1 ~ 1005.1 m^2/g) and the pore size ranging from 3.7 nm to 4.6 nm.

Figure 2.

Table 1

3.2 Solid-state NMR investigation

The investigation of the local structure and acidity of U-[Al]MCM-41 materials is of great importance for understanding their behavior in the Beckmann rearrangement of CHO. It has been widely accepted that the surface acidity of [Al]MCM-41 is generated by Al incorporated into the silica framework [25, 40, 41]. In typical MCM-41, three signals of Q^4 ($Si(OSi)_4$) (δ_{29Si} = -109 ppm), Q^3 ($Si(OSi)_3OH$) (δ_{29Si} = -101 ppm) and Q^2 ($Si(OSi)_2(OH)_2$) (δ_{29Si} = -92 ppm) species were often observed in the silica framework [25], similar as shown in the simulation of ^{29}Si MAS NMR spectra (Fig. 3). Additional Si(1Al) signals at δ_{29Si} = -101 ppm overlapes with Q^3 ($Si(OSi)_3OH$) signals were also observed. Si(1Al) signal has been attributed to aluminum atoms incorporated into the silica framework and coordinated to silicon atoms [54], contributing to the increase of (Q^3 + Si(1Al)) signal with decreasing the Si/Al ratio [25], e.g. 22 % for U-[Al]MCM-41/50 *vs.* 30 % for U-[Al]MCM-41/10.

Figure 3.

^{27}Al MAS NMR spectroscopy has been applied to investigate Al species incorporated into the silica framework. All spectra of current U-[Al]MCM-41 materials are dominated by signals of tetrahedrally coordinated aluminum (Al^{IV}) species at δ_{27Al} = 54 ppm, while weak signals at δ_{27Al} = 0 ppm and a small hump at δ_{27Al} = 28 ppm (only observed with U-[Al]MCM-41/10) are due to octahedrally coordinated aluminum (Al^{VI}) and pentahedrally coordinated aluminum (Al^{V})species, respectively (Fig. 4) [40, 55]. Al^{VI} species is often associated with surface Lewis acidity, and possibly enhanced with increasing the Al^{IV} content [25]. Al^{IV} is well known as Al species incorporated into the silica framework, which is able to enhance the acid strength of neighboring SiOH groups to form BAS [25, 40, 41]. With decreasing the Si/Al ratio from 50 to 10, the Al^{IV} signal is strongly enhanced. This indicates an increasing number of Al atoms (Al^{VI}) are incorporated into the silica framework, and result in more BAS on U-[Al]MCM-41 surface.

Figure 4.

^{1}H MAS NMR spectra is a powerful tool in the identification and quantification of these surface acidic protons [40]. As shown in Fig. 5, the ^{1}H MAS NMR spectra of dehydrated U-[Al]MCM-41 materials are dominated by a strong peak at δ_{1H} = 1.8 ppm. No obvious low-field signals of acidic OH groups can be detected, such as strong acidic bridging OH groups in dehydrated zeolites is often probed at δ_{1H} =

3.6-4.3 ppm [40]. Adsorption of a strong base (e.g. ammonia) on a dehydrated sample is a suitable method to identify surface OH groups with enhanced strength [40]. After evacuation of weakly adsorbed ammonia on dehydrated U-[Al]MCM-41 (Fig. 5 a-e top), the appearance of a new signal at δ_{1H} = 6.7 ppm indicates the formation of ammonium ions via ammonia protonation at surface acid sites. The intensity of ammonium ions can be utilized to evaluate the density of acidic OH groups on the surface [40, 56]. The quantitative results of U-[Al]MCM-41 materials were summarized in Table 2. The density (from 10.4×10^{-2} to 21.3×10^{-2} mmol/g) of BAS were enhanced with decreasing Si/Al ratio from 50 to 10, in line with more Al atoms (Al^{VI}) are incorporated into the silica framework as observed in Fig. 4.

Figure 5.

Table 2

The strength of BAS on U-[Al]MCM-41 were further evaluated by ^{13}C MAS NMR spectroscopy using acetone-2-^{13}C as a probe molecule [40]. As a scale, a larger low-field δ_{13C} shift represents a higher strength of BAS. As shown in Fig. 6, the spectra of all U-[Al]MCM-41 materials were dominated by a signal δ_{13C} = ca. 215 ppm. It indicates the acid strength of U-[Al]MCM-41 materials is independent of the Si/Al ratio as reported for [Al]MCM-41 previously [25], which is much weaker than acidic bridging OH groups (SiOHAl) in zeolites, e.g. δ_{13C} = 225 ppm for zeolite H-ZSM-5 [40]. This is because the BAS stegnth originates from the SiOH in the

vicnity of Al center in the local structure due to the amorphous nature of U-[Al]MCM-41, compared to crystalline zeolites that the strength of BAS strongly depends on the mean electronegativity determined by the framework Si/Al ratios [57, 58]. In addition, a weak signal at ca. 29 ppm was also observed, which can be assigned to the non-enriched methyl groups. No signal at δ_{13C} = ca. 229 ppm assigned to surface LAS can be detected in U-[Al]MCM-41, but was observed in [Al]MCM-41 previously [25]. This indicates that less LAS were formed because of the polymerization between Al species was inhibited under ultrasonic irradiation.

Figure 6.

In comparison with [Al]MCM-41 prepared without ultrasonic irradiation [4, 25, 41, 59-67], U-[Al]MCM-41 catalysts exhibit much higher (up to 12 times) BAS density at the similar Si/Al ratios (Table 2). Under ultrasonic irradiation, the acoustic vibrations pass through the liquid, resulting in strong agitation to generate smaller silicon and aluminum oligomers homogeneously dispersed in the mixture. It can facilitate the hydrolysis of TEOS and the formation of surfactant–silicate interface [48] to enhance the condensation between silica species with a higher Q^4 concentration, e.g. U-[Al]MCM-41/10 obtained a similar Q^4 concentration to [Al]MCM-41/30 (60 %) with three times higher Al addition (normally, higher Al content corresponding to lower Q^4). In the meanwhile, U-[Al]MCM-41 materials possess 2-8 times higher BAS density than these of [Al]MCM-41 prepared at the same conditions without ultrasonic

irradiation with similar Al^{IV}/Al^{VI} ratios at corresponding Si/Al ratios. This demonstrates the acoustic cavitation can inhibit the Al polymerization in the precursor, which benefits the formation and dispersion of smaller alumina oligomers into the silica framework, as a consequence, to improve the Al distribution into the silica framework. This is further evidenced by U-[Al]MCM-41/50 (10.4×10^{-2} mmol/g) obtained a similar BAS density to [Al]MCM/20 (10.1×10^{-2} mmol/g) with 2.5 times higher Al content, which indicates ultrasonic enhanced techniques can not only promote the formation of BAS, but also improve utilization of the Al precursor. Moreover, the BAS strength on U-[Al]MCM-41 (δ_{13C} = 215 ppm) is higher than these reported for [Al]MCM-41 (δ_{13C} = ca. 212-213 ppm) prepared at the same conditions without ultrasonic irradication [25]. This often hints a stronger interaction (or shorter distance) between Al and neighboring SiOH groups [68, 69], which may be caused by the ultrasonic irradiation improvement of the condensation and rearrangement of Al in the local structure of SiOH. Therefore, ultrasonic enhanced preparation can enhance both the density and strength of surface BAS on [Al]MCM-41 materials.

3.3 Beckmann rearrangement of cyclohexanone oxime (CHO) to ε-caprolactam (CPL)

The catalytic Beckmann rearrangement of CHO in PhCN to CPL over U-[Al]MCM-41 catalysts (dehydrated at 393 K) was carried out at 393 K for 7 h. The conversions of CHO and selectivity of CPL obtained over U-[Al]MCM-41 catalysts are shown as a function of reaction time dehydrated at 393 K in Fig. 7 and the reaction results are summarized in Table 3. The conversion of CHO started

immediately with U-[Al]MCM-41/50 having lowest Al content. Decreasing Si/Al ratio strikingly enhanced the conversion of CHO from 49.4 % for U-[Al]MCM-41/50 to 94.9 % for U-[Al]MCM-41/10. In the meanwhile, the selectivity of CPL increased from 49.2 % for U-[Al]MCM-41/50 to 63 % for U-[Al]MCM-41/10.

Figure 7

Table 3

Increasing both the CHO conversion and selectivity to CPL correlates well to enhancement of BAS density from 10.4×10^{-2} to 21.3×10^{-2} mmol/g with decreasing the Si/Al ratio. It is quite different from gas-phase Beckmann rearrangement, where weak acidic SiOH groups are considerably more active than BAS [3, 70-72]. This has been attributed to the high temperature (> 573 K) required for CPL desorption from BAS sites [27, 73] is enough to overcome the energy barrier for the reaction over SiOH groups. However, U-[Al]MCM-41 (Si/Al ≥ 30) having a higher total SiOH density of 3.5-3.84 mmol/g, obtained a much lower catalytic performance than that of U-[Al]MCM-41 (Si/Al = 10-20) having a SiOH density of only 2.1-2.3 mmol/g. This indicates more weakly acidic SiOH groups was less active than BAS for liquid-phase Beckmann rearrangement under moderate temperature as that reported earlier [8]. On the other hand, BAS with higher acid strength than SiOH is able to covert CHO into CPL [6-8, 14], while CPL can be smoothly removed from BAS at moderate temperature with suitable solvent, e.g. PhCN. Therefore, the catalytic performance of

U-[Al]MCM-41 catalysts can be significantly improved by increasing the BAS density, except for U-[Al]MCM-41/20. It has been observed that U-[Al]MCM-41/20 having similar density of BAS (11×10^{-2} mmol/g) but much lower SiOH density (2.1 mmol/g) than U-[Al]MCM-41/50, yielded a 32.3 % higher CHO conversion and 12.9 % higher CPL selectivity.

Since the conversion of CHO and desorption of CPL are both influenced by the acid strength of surface sites, the effects of BAS and SiOH groups on Beckmann rearrangement were further evaluated by the ratio of BAS/(weakly acidic SiOH groups) as shown in Table 2. This ratio increased from 3 % - 9.3 % with decreasing Si/Al ratio from 50 to 10, which is consistent with the enhanced catalytic performance for all U-[Al]MCM-41 catalysts. Particularly in the comparison of U-[Al]MCM-41/20 with U-[Al]MCM-41/30, the latter has 1.5 and 1.8 times higher density of BAS and SiOH groups, respectively, but obtained 22.1 % and 7.8 % lower CHO conversion and CPL selectivity, respectively. It worth to point out that the increase of CPL selectivity correlates with increasing the (BAS/weakly acidic SiOH groups) ratio. Weakly acidic SiOH groups are active sites in gas-phase Beckmann rearrangement. At the high temperature (> 573 K), the weak strength of SiOH groups is sufficient to perform the rearrangement, and facilitates the CPL desorption to improve the catalytic performance, compared to BAS. However, these weakly acidic SiOH groups are not so active for Beckmann rearrangement at moderate temperature (303 K) [8], instead, they promote the conversion of CHO into cyclohexanone as the major by-product [74] that can be detected here. Therefore, the catalytic performance of these

U-[Al]MCM-41 catalysts can be significantly improved with a higher concentration of BAS.

The catalytic behavior of U-[Al]MCM-41 catalysts was further investigated under different dehydration temperatures, since physisorbed water molecules can be gradually removed and uncover surface SiOH groups with increasing dehydration temperature [75]. Here, the catalytic performances of U-[Al]MCM-41/10 and U-[Al]MCM-41/30 dehydrated at 393 and 473 K respectively, as a function of time were depicted as shown in Fig. 8. Obviously, catalysts dehydrated at 393 K provides a 2.3 times higher CHO conversion (94.9 % vs. 41.8 % for U-[Al]MCM-41/10 and 60.1 % vs. 25.4 % for U-[Al]MCM-41/30) and two times higher yield of CPL (59.8 % vs. 29.3 % for U-[Al]MCM-41/10 and 32.4 % vs. 17.4 % for U-[Al]MCM-41/30) than that of catalysts dehydrated at 473 K. In comparison, the reaction over non-activated U-[Al]MCM-41/10 obtained a CHO conversion of 45.3 % and CPL yield of 13.1 %. It indicates removing weakly adsorbed bulk water at low temperature (e.g. 393 K) can improve the accessibility of reactant to surface active sites, while hydrogen-bonded water molecules desorbed at high temperature (e.g. 473 K) may release more SiOH groups for side reactions.

Figure 8.

Finally, the reusability of the U-[Al]MCM-41 catalysts was tested with the best-performing catalyst U-[Al]MCM-41/10. After each test, U-[Al]MCM-41/10 was

recovered by calcined in air at 823 K. As shown in Fig. 9, recycling the catalyst five times did not lead to a significant loss of activity (conversion kept at ca. 100 %) and selectivity to lactam (63-65.1 %). This indicates U-[Al]MCM-41 catalysts are stable for Beckmann rearrangement at current conditions.

Figure. 9

4. Conclusions

In this work, a series of U-[Al]MCM-41 catalysts with various Si/Al ratios (10-50) were prepared under ultrasonic irradiation. ^{27}Al and ^{29}Si MAS NMR investigations (Fig. 4 and 5) showed increasing number of Al atoms incorporated into the silica framework of U-[Al]MCM-41 catalysts with Si/Al ratio decreased. It leads to the strong increase of BAS density (from 10.4 to 21.3×10^{-2} mmol/g, Table 2), quantified by ^{1}H MAS NMR spectroscopy with NH_3 as probe molecules (Fig. 3), which is 2-8 time higher than that (1.3 to 12.1×10^{-2} mmol/g) of [Al]MCM-41 prepared at the same conditions but without ultrasonic irradiation, and up to 12 times higher BAS density than [Al]MCM-41 catalysts reported in the literature [4, 25, 41, 59-67]. Under ultrasonic irradiation, the strong agitation results in smaller silicon and aluminum oligomers homogeneously dispersed in the mixture. It can also resist the polymerization of Al species and promote aluminum atoms incorporated into the silica framework to enhance the BAS density. These BAS exhibit higher strength than previous [Al]MCM-41 materials, scaled by ^{13}C MAS NMR spectroscopy using

acetone-2-^{13}C as a probe molecule (Fig. 6), which may be caused by ultrasonic irradiation improved the condensation between aluminum and silicon precursor.

In the liquid-phase Beckmann rearrangement of CHO, the catalytic performance of U-[Al]MCM-41 correlates well with higher BAS acidity, particularly with the increase in the BAS/(weakly acidic SiOH groups) ratio. Dehydration at relative low temperature (393 K *vs*. 473 K) can block the SiOH hydrogen-bonded to water molecules and suppress the side reaction for cyclohexanone. The highest CHO conversion (94.9 %) and CPL yield (59.8 %) were both obtained with U-[Al]MCM-41/10 dehydrated at 393 K and after 7 h reaction. U-[Al]MCM-41/10 provides the highest CPL yield (52.3 %) after 5 h reaction, which is ca. 10 % higher than the best [Al]MCM-41 reported hitherto at the similar conditions [8]. Therefore, this work provides an alternative way to further enhance the catalytic performance of solid acids in the Beckmann rearrangement reaction.

Acknowledgements

This work was supported by the Australian Research Council Discovery Projects (DP150103842), the Faculty's MCR Scheme, Energy and Materials Clusters and the Early Career Research Scheme and the Major Equipment Scheme from the University of Sydney. M.H. thanks for financial support by Deutsche Forschungsgemeinschaft and Baden-Württemberg Stiftung.

References

[1] J. Ritz, H. Fuchs, H. Kieczka, W.C. Moran, Caprolactam, Ullmann's Encyclopedia of Industrial Chemistry, Wiley-VCH Verlag GmbH & Co. KGaA,

2000.
[2] A. Corma, H. Garcia, J. Primo, E. Sastre, Beckmann rearrangement of cyclohexanone oxime on zeolites, Zeolites 11 (1991) 593-597.
[3] L. Forni, G. Fornasari, G. Giordano, C. Lucarelli, A. Katovic, E. Trifiro, C. Perri, J.B. Nagy, Vapor phase Beckmann rearrangement using high silica zeolite catalyst, Phys. Chem. Chem. Phys. 6 (2004) 1842-1847.
[4] T.D. Conesa, R. Mokaya, Z. Yang, R. Luque, J.M. Campelo, A.A. Romero, Novel mesoporous silicoaluminophosphates as highly active and selective materials in the Beckmann rearrangement of cyclohexanone and cyclododecanone oximes, J. Catal. 252 (2007) 1-10.
[5] N.C. Marziano, L. Ronchin, C. Tortato, A. Vavasori, C. Badetti, Catalyzed Beckmann rearrangement of cyclohexanone oxime in heterogeneous liquid/solid system Part 1: Batch and continuous operation with supported acid catalysts, J. Mol. Catal. A-Chem. 277 (2007) 221-232.
[6] N.C. Marziano, L. Ronchin, C. Tortato, A. Vavasori, M. Bortoluzzi, Catalyzed Beckmann rearrangement of cyclohexanone oxime in heterogeneous liquid/solid system Part 2: Influence of acid catalysts and organic promoters, J. Mol. Catal. A-Chem. 290 (2008) 79-87.
[7] G.G. Midyana, R.G. Makitra, E.Y. Pal'chikova, Solvent effect on the kinetics of Beckmann rearrangement, Russ. J. Gen. Chem. 80 (2010) 31-34.
[8] C. Ngamcharussrivichai, P. Wu, T. Tatsumi, Liquid-phase Beckmann rearrangement of cyclohexanone oxime over mesoporous molecular sieve catalysts, J. Catal. 227 (2004) 448-458.
[9] C. Ngamcharussrivichai, P. Wu, T. Tatsumi, Selective production of epsilon-caprolactam via liquid-phase Beckmann rearrangement of cyclohexanone oxime over HUSY catalyst, Chem. Lett. 33 (2004) 1288-1289.
[10] C. Ngamcharussrivichai, P. Wu, T. Tatsumi, Active and selective catalyst for liquid phase Beckmann rearrangement of cyclohexanone oxime, J. Catal. 235 (2005) 139-149.
[11] C. Ngamcharussrivichai, P. Wu, T. Tatsumi, Catalytically active and selective centers for production of epsilon-caprolactam through liquid phase Beckmann rearrangement over H-USY catalyst, Appl. Catal. A-Gen. 288 (2005) 158-168.
[12] J.J. Peng, Y.Q. Deng, Catalytic Beckmann rearrangement of ketoximes in ionic liquids, Tetrahedron Lett. 42 (2001) 403-405.
[13] N.R. Shiju, M. AnilKumar, W.F. Hoelderich, D.R. Brown, Tungstated zirconia catalysts for liquid-phase Beckmann rearrangement of cyclohexanone oxime: structure-activity relationship, J. Phys. Chem. C 113 (2009) 7735-7742.
[14] N.R. Shiju, H.M. Williams, D.R. Brown, Cs exchanged phosphotungstic acid as an efficient catalyst for liquid-phase Beckmann rearrangement of oximes, Appl. Catal. B-Environ. 90 (2009) 451-457.
[15] B. Thomas, U.R. Prabhu, S. Prathapan, S. Sugunan, Towards a green synthesis of isoquinoline: Beckmann rearrangement of E,-cinnamaldoxime over H-zeolites, Microporous Mesoporous Mater. 102 (2007) 138-150.
[16] B. Thomas, S. Prathapan, S. Sugunan, Solid acid-catalyzed

dehydration/Beckmann rearrangement of aldoximes: towards high atom efficiency green processes, Microporous Mesoporous Mater. 79 (2005) 21-27.

[17] W. Zhao, P. Salame, V. Herledan, F. Launay, A. Gedeon, T. Qi, Study the liquid-phase Beckmann rearrangement on the surface of SBA-15-SO_3H catalyst, J. Porous Mater. 17 (2010) 335-340.

[18] X.G. Wang, C.C. Chen, S.Y. Chen, Y. Mou, S.F. Cheng, Arenesulfonic acid functionalized mesoporous silica as a novel acid catalyst for the liquid phase Beckmann rearrangement of cyclohexanone oxime to epsilon-caprolactam, Appl. Catal. A-Gen. 281 (2005) 47-54.

[19] K. Chaudhari, R. Bal, A.J. Chandwadkar, S. Sivasanker, Beckmann rearrangement of cyclohexanone oxime over mesoporous Si-MCM-41 and Al-MCM-41 molecular sieves, J. Mol. Catal. A-Chem. 177 (2002) 247-253.

[20] A.-B. Fernandez, A. Marinas, T. Blasco, V. Fornes, A. Corma, Insight into the active sites for the Beckmann rearrangement on porous solids by in situ infrared spectroscopy, J. Catal. 243 (2006) 270-277.

[21] A.N. Ko, C.C. Hung, C.W. Chen, K.H. Ouyang, Mesoporous molecular sieve Al-MCM-41 as a novel catalyst for vapor-phase Beckmann rearrangement of cyclohexanone oxime, Catal. Lett. 71 (2001) 219-224.

[22] P. O'Sullivan, L. Forni, B.K. Hodnett, The role of acid site strength in the Beckmann rearrangement, Ind. & Eng. Chem. Res. 40 (2001) 1471-1475.

[23] T.D. Conesa, J.M. Hidalgo, R. Luque, J.M. Campelo, A.A. Romero, Influence of the acid-base properties in Si-MCM-41 and B-MCM-41 mesoporous materials on the activity and selectivity of epsilon-caprolactam synthesis, Appl. Catal. A-Gen. 299 (2006) 224-234.

[24] M. Anilkumar, W.F. Hoelderich, Highly active and selective Nb modified MCM-41 catalysts for Beckmann rearrangement of cyclohexanone oxime to epsilon-caprolactam, J. Catal. 260 (2008) 17-29.

[25] Z. Wang, Y. Jiang, R. Rachwalik, Z. Liu, J. Shi, M. Hunger, J. Huang, One-step room-temperature synthesis of [Al]-MCM-41 materials for the catalytic conversion of phenylglyoxal to ethylmandelate, ChemCatChem 5 (2013) 3889-3896.

[26] A.B. Fernandez, M. Boronat, T. Blasco, A. Corma, Establishing a molecular mechanism for the Beckmann rearrangement of oximes over microporous molecular sieves, Angew. Chem.-Int. Ed. 44 (2005) 2370-2373.

[27] H. Sato, K. Hirose, Y. Nakamura, FTIR study of the Beckmann rearrangement over pentasil-type zeolite, Chem. Lett. (1993) 1987-1990.

[28] T. Takahashi, K. Ueno, T. Kai, Vapor-phase reaction of cyclohexanone oxime over boria modified HSZM-5 zeolites, Canadian J. Chem. Eng. 69 (1991) 1096-1099.

[29] C.T. Kresge, M.E. Leonowicz, W.J. Roth, J.C. Vartuli, J.S. Beck, Ordered mesoporous molecular-sieves synthesized by a liquid-crystal template mechanism, Nature 359 (1992) 710-712.

[30] J.S. Beck, J.C. Vartuli, W.J. Roth, M.E. Leonowicz, C.T. Kresge, K.D. Schmitt, C.T.W. Chu, D.H. Olson, E.W. Sheppard, S.B. McCullen, J.B. Higgins, J.L.

Schlenker, A new family of mesoporous molecular-sieves prepared with liquid-crystal templates, J. Am. Chem. Soc. 114 (1992) 10834-10843.

[31] G. Lelong, S. Bhattacharyya, S. Kline, T. Cacciaguerra, M.A. Gonzalez, M.L. Saboungi, Effect of surfactant concentration on the morphology and texture of MCM-41 materials, J. Phys. Chem. C 112 (2008) 10674-10680.

[32] S.N. Che, S.Y. Lim, M. Kaneda, H. Yoshitake, O. Terasaki, T. Tatsumi, The effect of the counteranion on the formation of mesoporous materials under the acidic synthesis process, J. Am. Chem. Soc. 124 (2002) 13962-13963.

[33] M. Grun, K.K. Unger, A. Matsumoto, K. Tsutsumi, Novel pathways for the preparation of mesoporous MCM-41 materials: control of porosity and morphology, Microporous Mesoporous Mater. 27 (1999) 207-216.

[34] Q. Cai, W.Y. Lin, F.S. Xiao, W.Q. Pang, X.H. Chen, B.S. Zou, The preparation of highly ordered MCM-41 with extremely low surfactant concentration, Microporous Mesoporous Mater. 32 (1999) 1-15.

[35] P. Verlooy, A. Aerts, O.I. Lebedev, G. Van Tendeloo, C. Kirschhock, J.A. Martens, Synthesis of highly stable pure-silica thin-walled hexagonally ordered mesoporous material, Chem. Commun. (2009) 4287-4289.

[36] Y.M. Setoguchi, Y. Teraoka, I. Moriguchi, S. Kagawa, N. Tomonaga, A. Yasutake, J. Izumi, Rapid Room Temperature synthesis of hexagonal mesoporous silica using inorganic silicate sources and cationic surfactants under highly acidic conditions, J. Porous Mater. 4 (1997) 129-134.

[37] F.J. Romero, C. Jiménez, I. Huc, R. Oda, Room temperature synthesis of ordered porous silicas templated by symmetric and dissymmetric gemini surfactants $[C_nH_{2n+1}N(CH_3)_2(CH_2)_2(CH_3)_2NC_mH_{2m+1}]Br_2$, Microporous Mesoporous Mater. 69 (2004) 43-48.

[38] M. Grun, I. Lauer, K.K. Unger, The synthesis of micrometer- and submicrometer-size spheres of ordered mesoporous oxide MCM-41, Adv. Mater. 9 (1997) 254-&.

[39] Q. Cai, Z.S. Luo, W.Q. Pang, Y.W. Fan, X.H. Chen, F.Z. Cui, Dilute solution routes to various controllable morphologies of MCM-41 silica with a basic medium, Chem. Mater. 13 (2001) 258-263.

[40] Y. Jiang, J. Huang, W. Dai, M. Hunger, Solid-state nuclear magnetic resonance investigations of the nature, property, and activity of acid sites on solid catalysts, Solid State Nucl. Magn. Reson., 39 (2011) 116-141.

[41] Q. Luo, F. Deng, Z.Y. Yuan, J. Yang, M.J. Zhang, Y. Yue, C.H. Ye, Using trimethylphosphine as a probe molecule to study the acid states in Al-MCM-41 materials by solid-state NMR spectroscopy, J. Phys. Chem. B, 107 (2003) 2435-2442.

[42] A. Matsumoto, H. Chen, K. Tsutsumi, M. Grun, K. Unger, Novel route in the synthesis of MCM-41 containing framework aluminum and its characterization, Microporous Mesoporous Mater. 32 (1999) 55-62.

[43] G.A. Eimer, L.B. Pierella, G.A. Monti, O.A. Anunziata, Synthesis and characterization of Al-MCM-41 and Al-MCM-48 mesoporous materials, Catal. Lett. 78 (2002) 65-75.

[44] K.S. Suslick, S.B. Choe, A.A. Cichowlas, M.W. Grinstaff, Sonochemical synthesis of amorphous iron, Nature 353 (1991) 414-416.
[45] J.J. Zhu, Y. Koltypin, A. Gedanken, General sonochemical method far the preparation of nanophasic selenides: Synthesis of ZnSe nanoparticles, Chem. Mater. 12 (2000) 73-78.
[46] K.S. Suslick, Sonochemistry, Science 247 (1990) 1439-1445.
[47] K.S. Suslick, G.J. Price, Applications of ultrasound to materials chemistry, Annual Rev. Mater. Sci. 29 (1999) 295-326.
[48] X.H. Tang, S.W. Liu, Y.Q. Wang, W.P. Huang, E. Sominski, O. Palchik, Y. Koltypin, A. Gedanken, Rapid synthesis of high quality MCM-41 silica with ultrasound radiation, Chem. Commun. (2000) 2119-2120.
[49] X.H. Tang, X. Wen, W.P. Huang, S.W. Liu, Y.Q. Wang, O. Palchik, Y. Koltypin, D.M. Pickup, E.R.H. van Eck, A. Gedanken, Novel synthesis of ordered MCM-41 titanosilicates with very high titanium content via ultrasound radiation, Isr. J. Chem., 44 (2004) 235-241.
[50] N.T. Mathew, S. Khaire, S. Mayadevi, R. Jha, S. Sivasanker, Rearrangement of allyl phenyl ether over Al-MCM-41, J. Catal. 229 (2005) 105-113.
[51] Z.H. Luan, C.F. Cheng, W.Z. Zhou, J. Klinowski, Mesopore molecular-sieve MCM-41 containing framework aluminum, J. Phys. Chem. 99 (1995) 1018-1024.
[52] X.Y. Chen, L.M. Huang, G.Z. Ding, Q.Z. Li, Characterization and catalytic performance of mesoporous molecular sieves Al-MCM-41 materials, Catal. Lett. 44 (1997) 123-128.
[53] K.S.W. Sing, D.H. Everett, R.A.W. Haul, L. Moscou, R.A. Pierotti, J. Rouquerol, T. Siemieniewska, Reporting physisorption data for gas solid systems with special reference to the determination of surface-area and porosity (Recommendations 1984), Pure Appl. Chem. 57 (1985) 603-619.
[54] M. Hunger, Solid-State NMR Spectroscopy, in: E.G.D. A.W. Chester (Ed.) Zeolite Characterization and Catalysis - A Tutorial, Springer, Heidelberg, 2009, pp. 82.
[55] Z.H. Luan, C.F. Cheng, H.Y. He, J. Klinowski, Thermal-stability of structural aluminum in the mesoporous molecular-sieve MCM-41, J. Phys. Chem., 99 (1995) 10590-10593.
[56] J. Huang, N. van Vegten, Y. Jiang, M. Hunger, A. Baiker, Increasing the Bronsted acidity of flame-derived silica/alumina up to zeolitic strength, Angew. Chem.-Int. Ed. 49 (2010) 7776-7781.
[57] P.A. Jacobs, W.J. Mortier, J.B. Uytterhoeven, Properties of zeolites in relation to their electronegativity - acidity, carboniogenic activity and strength of interaction in transition-metal complexes, J. Inorg. & Nucl. Chem. 40 (1978) 1919-1923.
[58] W.J. Mortier, Zeolite electronegativity related to physicochemical properties, J. Catal. 55 (1978) 138-145.
[59] L.Y. Chen, Z. Ping, G.K. Chuah, S. Jaenicke, G. Simon, A comparison of post-synthesis alumination and sol-gel synthesis of MCM-41 with high

framework aluminum content, Microporous Mesoporous Mater., 27 (1999) 231-242.
[60] H. Ziaei-Azad, A. Sayari, Bifunctional MCM-41 aluminosilicate supported Ir with adjusted metal and acid functionality for catalytic ring opening of 1,2-dimethylcyclohexane, J. Catal., 344 (2016) 729-740.
[61] R. Locus, D. Verboekend, R. Zhong, K. Houthoofd, T. Jaumann, S. Oswald, L. Giebeler, G. Baron, B.F. Sels, Enhanced Acidity and Accessibility in Al-MCM-41 through aluminum activation, Chem. Mater., 28 (2016) 7731-7743.
[62] V.B.F. Custodis, S.A. Karakoulia, K.S. Triantafyllidis, J.A. van Bokhoven, Catalytic fast pyrolysis of lignin over high-surface-area mesoporous aluminosilicates: effect of porosity and acidity, ChemSusChem, 9 (2016) 1134-1145.
[63] B. Lindlar, A. Kogelbauer, R. Prins, Chemical, structural, and catalytic characteristics of Al-MCM-41 prepared by pH-controlled synthesis, Microporous Mesoporous Mater., 38 (2000) 167-176.
[64] M. Xu, W. Wang, M. Seiler, A. Buchholz, M. Hunger, Improved Brønsted acidity of mesoporous [Al]MCM-41 material treated with ammonium fluoride, J. Phys. Chem. B, 106 (2002) 3202-3208.
[65] X. Chen, M. Jia, G. Liu, X. Zhang, L. Wang, Z. Mi, Catalytic performance of grafted Al-MCM-41 in hydroisomerization of n-dodecane, Appl. Surf. Sci., 256 (2010) 5856-5861.
[66] I. Jiménez-Morales, M. Moreno-Recio, J. Santamaría-González, P. Maireles-Torres, A. Jiménez-López, Production of 5-hydroxymethylfurfural from glucose using aluminium doped MCM-41 silica as acid catalyst, Appl. Catal. B: Environ., 164 (2015) 70-76.
[67] K.-Y. Kwak, M.-S. Kim, D.-W. Lee, Y.-H. Cho, J. Han, T.S. Kwon, K.-Y. Lee, Synthesis of cyclopentadiene trimer (tricyclopentadiene) over zeolites and Al-MCM-41: The effects of pore size and acidity, Fuel, 137 (2014) 230-236.
[68] C. Chizallet, P. Raybaud, Pseudo-bridging silanols as versatile Brønsted acid sites of amorphous aluminosilicate surfaces, Angew. Chem.-Int. Ed., 48 (2009) 2891-2893.
[69] U. Eichler, M. Brandle, J. Sauer, Predicting absolute and site specific acidities for zeolite catalysts by a combined quantum mechanics interatomic potential function approach, J. Phys. Chem. B, 101 (1997) 10035-10050.
[70] B. Bonelli, L. Forni, A. Aloise, J.B. Nagy, G. Fornasari, E. Garrone, A. Gedeon, G. Giordano, F. Trifiro, Beckmann rearrangement reaction: About the role of defect groups in high silica zeolite catalysts, Microporous Mesoporous Mater., 101 (2007) 153-160.
[71] H. Sato, K. Hirose, M. Kitamura, Vapor-phase beckmann rearrangement over highly silicious ZSM-5 .2. relations between the zeolitic properties of ZSM-5 and its catalytic activities for a vapor-phase Beckmann rearrangement, Nippon Kagaku Kaishi, (1989) 548-554.
[72] V.R.R. Marthala, Y. Jiang, J. Huang, W. Wang, R. Glaser, M. Hunger, Beckmann rearrangement of N-15-cyclohexanone oxime on zeolites silicalite-1, H-ZSM-5,

and H- B ZSM-5 studied by solid-state NMR spectroscopy, J. Am. Chem. Soc. 128 (2006) 14812-14813.

[73] V.R.R. Marthala, J. Frey, M. Hunger, Accessibility and interaction of surface OH groups in microporous and mesoporous catalysts applied for vapor-phase Beckmann rearrangement of oximes, Catal. Lett., 135 (2010) 91-97.

[74] M.A. Camblor, A. Corma, H. Garcia, V. Semmer-Herledan, S. Valencia, Active sites for the liquid-phase Beckmann rearrangement of cyclohexanone, acetophenone and cyclododecanone oximes, catalyzed by beta zeolites, J. Catal. 177 (1998) 267-272.

[75] L.T. Zhuravlev, The surface chemistry of amorphous silica. Zhuravlev model, Colloid Surf. A-Physicochem. Eng. Asp., 173 (2000) 1-38.

Tables

Table 1. BET surface areas, total pore volume, average pore diameters and the number of SiOH groups of U-[Al]MCM-41 materials.

	BET surface area (m^2/g)	**Total pore volume (cm^3/g)**	**Average pore diameter (nm)**
U-[Al]MCM-41/50	993.7	0.95	3.8
U-[Al]MCM-41/40	950.2	1.04	4.2
U-[Al]MCM-41/30	1005.1	0.92	3.7
U-[Al]MCM-41/20	962.3	0.88	3.7
U-[Al]MCM-41/10	887.1	1.02	4.6

Table 2. Concentrations and fractions of acidic OH groups of U-[Al]MCM-41 materials with different Si/Al ratio.

Si/Al ratios	Samples	Total SiOH groups[a] mmol/g	BAS[b] $\times 10^{-2}$ mmol/g	BAS/ weakly acidic SiOH %	Ref.
>50	U-[Al]MCM-41/50	3.5	10.4	3	
	[Al]MCM/50[c]	1.9	1.3		
	Other works		2.8-3.4		[41, 59]
40-49	U-[Al]MCM-41/40	3.9	13.6	3.5	
	[Al]MCM/40[c]	2.6	5.8		
	Other works		1.1-5.3		[60-62]
30-39	U-[Al]MCM-41/30	3.84	16	4.2	
	[Al]MCM/30[c]	2.9	7		
	Other works		9.1-15		[4, 62, 63]
20-29	U-[Al]MCM-41/20	2.1	11	5.2	
	[Al]MCM/20[c]	3.3	10.1		
	Other works		5.6-6.1		[41, 60, 65]
<20	U-[Al]MCM-41/10	2.3	21.3	9.3	
	[Al]MCM/10[c]	3.3	12.7		
	[Al]MCM/15[c]	3.4	12.1		
	Other works		7.1-19.8		[41, 59, 64-67]

[a] Total number of SiOH groups were obtained from quantitative ^{1}H MAS NMR experiments.

[b] BAS represents acidic SiOH groups generated by SiOH having neighboring Al species.

[c] The data for [Al]MCM-41 prepared at the same conditions without ultrasonication were taken from ref. [25].

Table 3. The catalytic reaction results in Beckmann rearrangement of cyclohexanone oxime to ε-caprolactam over U-[Al]MCM-41 with Si/Al ratio of 50, 40, 30, 20 and 10.[a]

Samples	Activation at 393 K			Activation at 473 K		
	C_{CHO}[b] %	S_{CPL}[b] %	Y_{CPL}[b] %	C_{CHO}[b] %	S_{CPL}[b] %	Y_{CPL}[b] %
[Al]MCM-41/50	49.9	49.2	24.6	30.5	73.0	22.3
[Al]MCM-41/40	54.3	53.2	28.9	25.6	53.4	13.7
[Al]MCM-41/30	60.1	54.3	32.6	25.4	68.6	17.4
[Al]MCM-41/20	82.2	62.1	51.0	30.3	61.1	18.5
[Al]MCM-41/10	94.9	63.0	59.8	41.8	70.1	29.3

[a] Conversion of cyclohexanone oxime (50 mg) in PhCN (10 ml) using 50 mg catalyst at 393 K for 7 h to yield ε-caprolactam.

[b] C_{CHO} = the conversion of cyclohexanone oxime (CHO), S_{CPL} = the selectivity to ε-caprolactam (CPL) and Y_{CPL} = the yield of CPL.

Figure Captions

Figure 1. Small angle XRD patterns of U-[Al]MCM-41/50, U-[Al]MCM-41/40, U-[Al]MCM-41/30, U-[Al]MCM-41/200 and U-[Al]MCM-41/10.

Figure 2. Nitrogen adsorption/desorption isotherms and pore size distribution of a) U-[Al]MCM-41/10, b) U-[Al]MCM-41/20, c) U-[Al]MCM-41/30, d) U-[Al]MCM-41/40 and e) U-[Al]MCM-41/50.

Figure 3. ^{29}Si MAS NMR spectra of U-[Al]MCM-41 with Si/Al = 10 (a) and 50 (b).

Figure 4. ^{27}Al MAS NMR spectra of U-[Al]MCM-41 with Si/Al = 10 (a), 20 (b), 30 (c), 40 (d) and 50 (e).

Figure 5. ^{1}H MAS NMR spectra of U-[Al]MCM-41 with Si/Al = 10 (a), 20 (b), 30 (c), 40 (d) and 50 (e) recorded before (bottom) and after (top) loading with NH_3 and subsequent evacuation of NH_3 loaded samples at 393 K for 1 h.

Figure 6. ^{13}C CP/MAS NMR spectra of U-[Al]MCM-41 of Si/Al = 40 (a) and 10 (b), recorded after dehydrated sample loading with acetone-2-^{13}C and subsequent evacuation of acetone-2-^{13}C loaded samples at room temperature for 20 min.

Figure 7. Catalytic conversion of CHO (a) and selectivity to CPL in the Beckmann rearrangement of CHO over U-[Al]MCM-41 with Si/Al = 10 (■), 20 (●), 30 (▲), 40 (◆)and 50 (★), dehydrated at 393 K.

Figure 8. Catalytic conversion of CHO (a) and selectivity to CPL in the Beckmann rearrangement of CHO (b) over U-[Al]MCM-41/10 (■) and U-[Al]MCM-41/30 (●), dehydrated at 393 K (close symbol) and 473 K (open symbol).

Figure 9. The conversion of oxime and selectivity of lactam after five recycling times

using U-[Al]MCM-41/10 under the standard conditions specified in Table 3 and the results obtained after 7 h reaction.

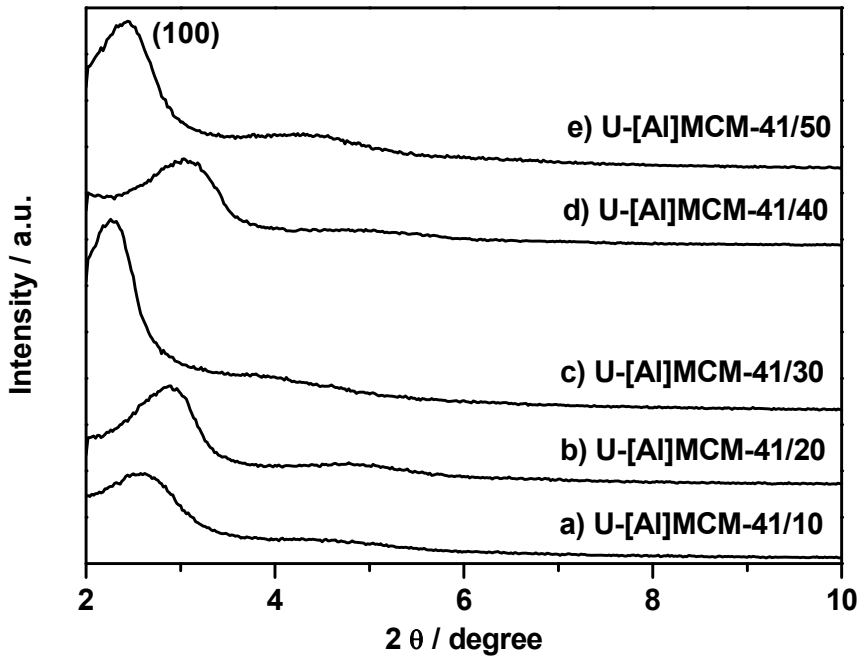
(100)
e) U-[Al]MCM-41/50
d) U-[Al]MCM-41/40
c) U-[Al]MCM-41/30
b) U-[Al]MCM-41/20
a) U-[Al]MCM-41/10
Intensity / a.u.
2
4
6
8
10
2 θ / degree

Fig. 1

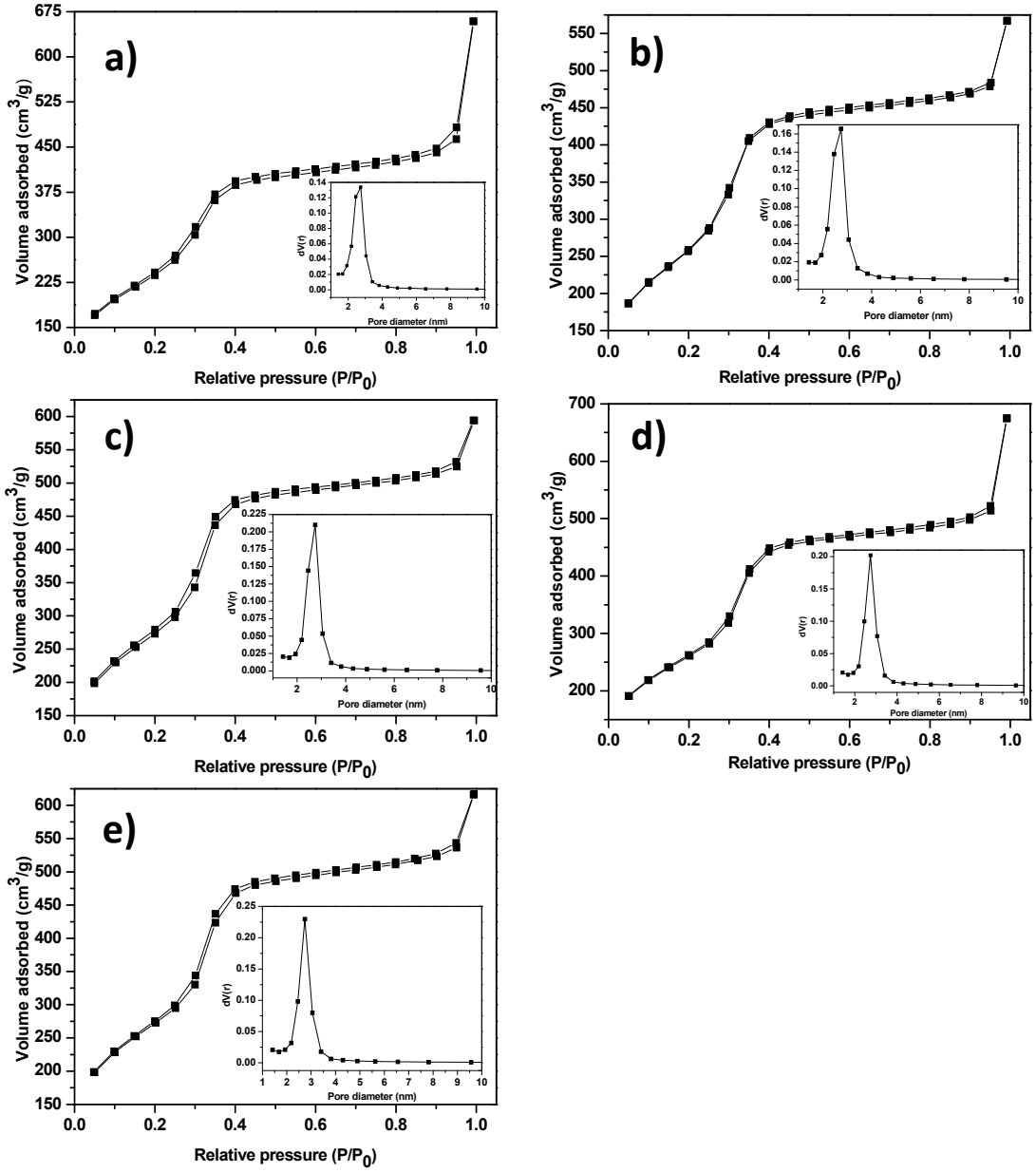
a)
b)
c)
d)
e)
Volume adsorbed (cm3/g)
Relative pressure (P/P0)
dV(r)
Pore diameter (nm)

Fig. 2

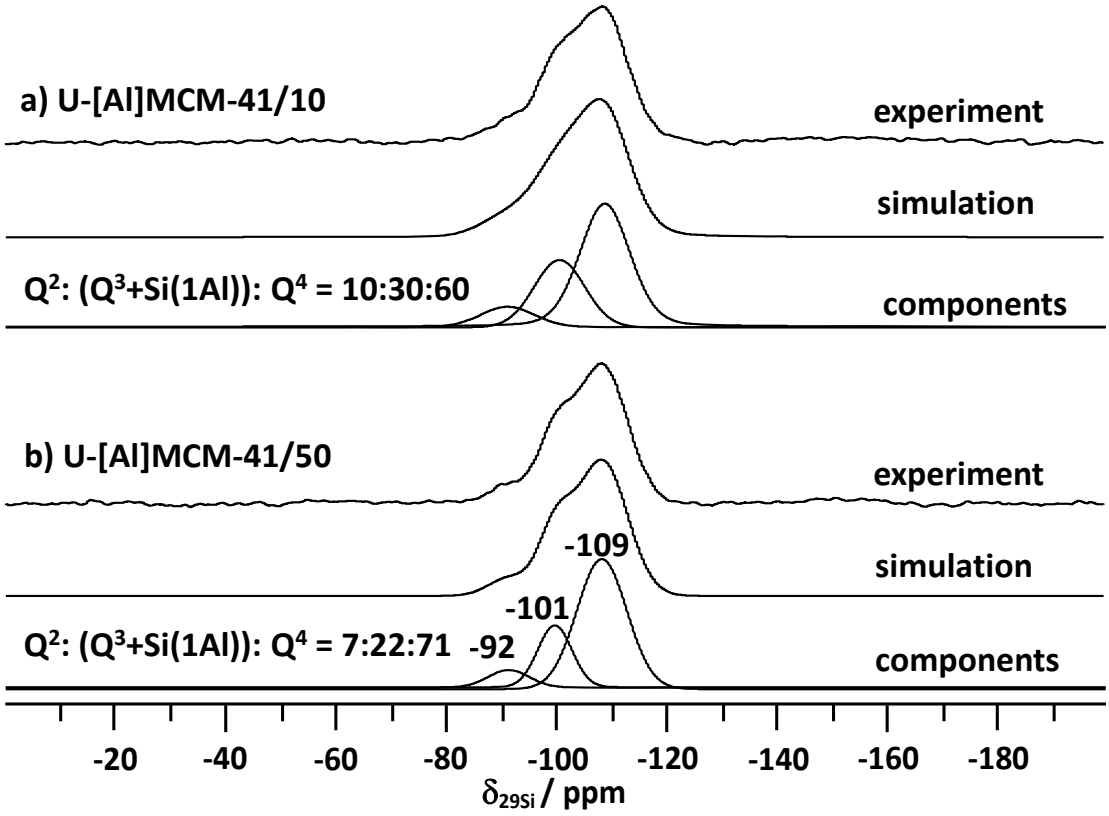
a) U-[Al]MCM-41/10
experiment
simulation
Q²: (Q³+Si(1Al)): Q⁴ = 10:30:60
components
b) U-[Al]MCM-41/50
experiment
-109
simulation
-101
Q²: (Q³+Si(1Al)): Q⁴ = 7:22:71 -92
components
-20
-40
-60
-80
-100
-120
-140
-160
-180
δ29Si / ppm

Fig. 3

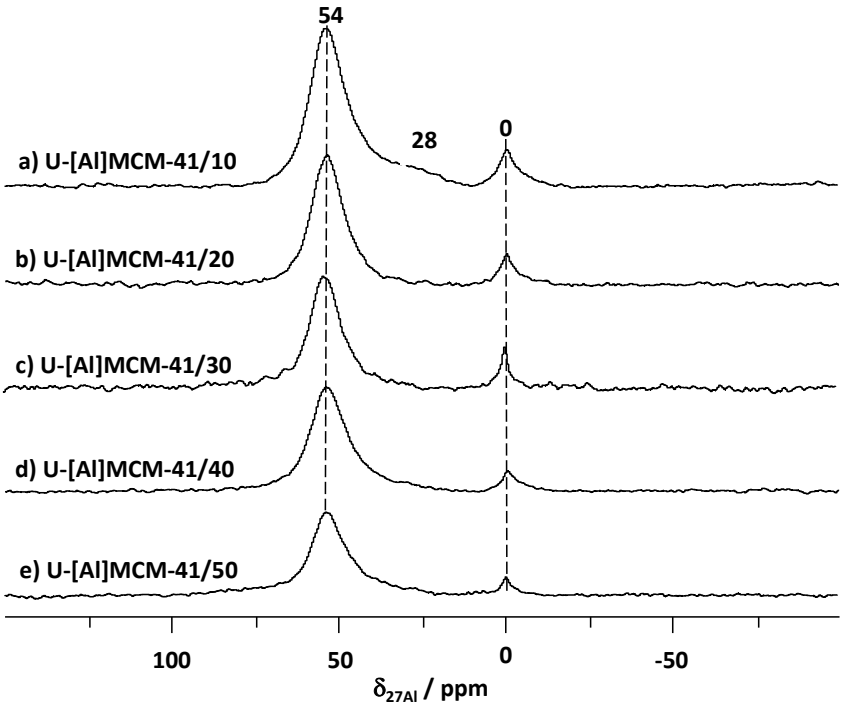
54
28
0
a) U-[Al]MCM-41/10
b) U-[Al]MCM-41/20
c) U-[Al]MCM-41/30
d) U-[Al]MCM-41/40
e) U-[Al]MCM-41/50
100
50
0
-50
δ27Al / ppm

Fig. 4

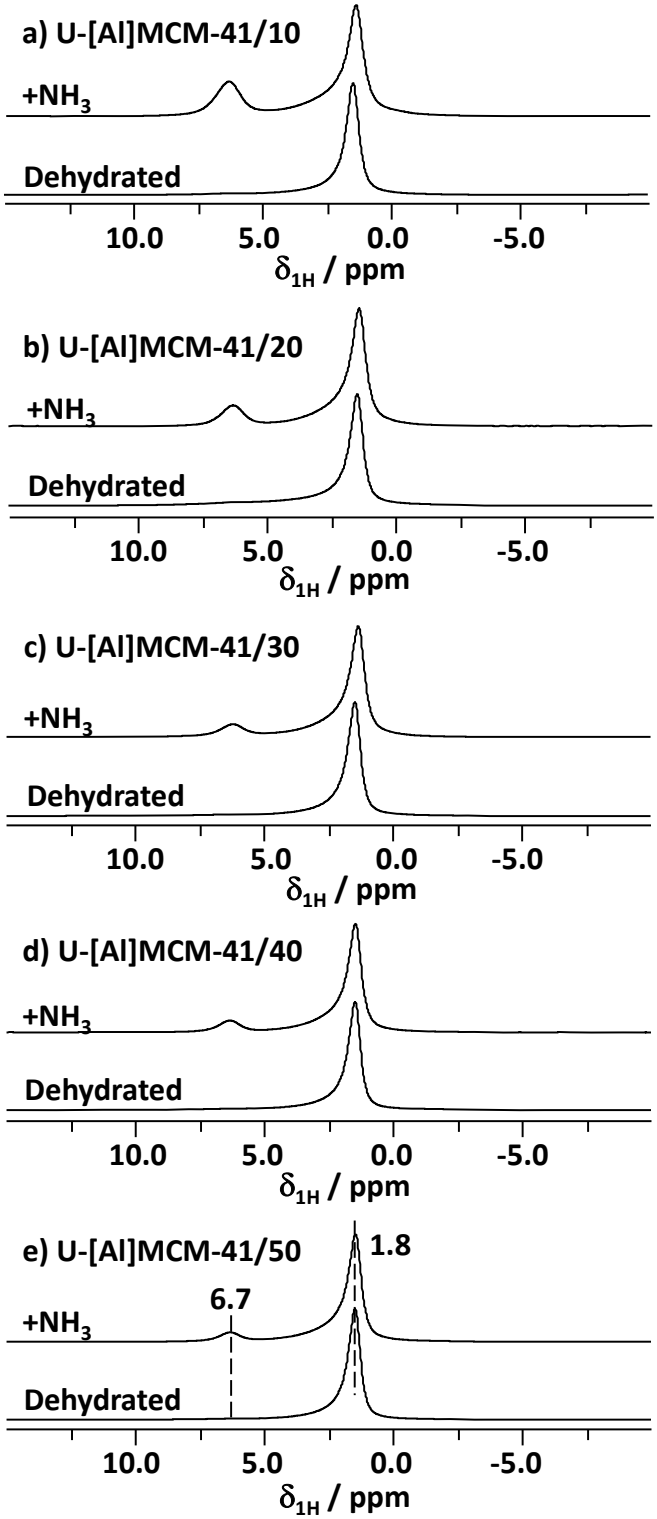
a) U-[Al]MCM-41/10
+NH3
Dehydrated
10.0
5.0
0.0
-5.0
δ1H / ppm
b) U-[Al]MCM-41/20
+NH3
Dehydrated
10.0
5.0
0.0
-5.0
δ1H / ppm
c) U-[Al]MCM-41/30
+NH3
Dehydrated
10.0
5.0
0.0
-5.0
δ1H / ppm
d) U-[Al]MCM-41/40
+NH3
Dehydrated
10.0
5.0
0.0
-5.0
δ1H / ppm
e) U-[Al]MCM-41/50
1.8
6.7
+NH3
Dehydrated
10.0
5.0
0.0
-5.0
δ1H / ppm

Fig. 5

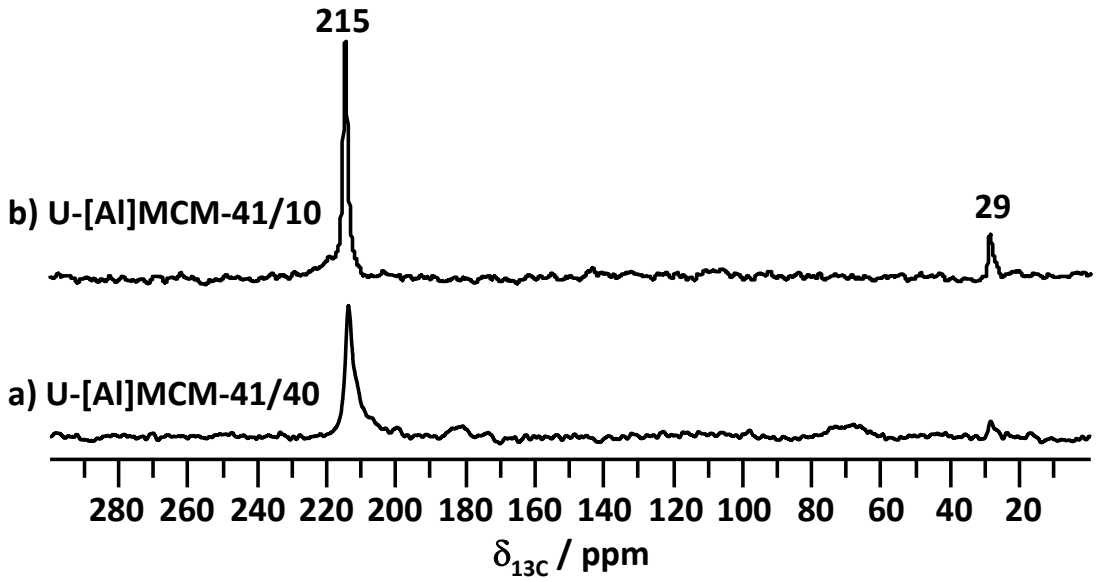
215
b) U-[Al]MCM-41/10
29
a) U-[Al]MCM-41/40
280 260 240 220 200 180 160 140 120 100 80 60 40 20
δ13C / ppm

Fig. 6

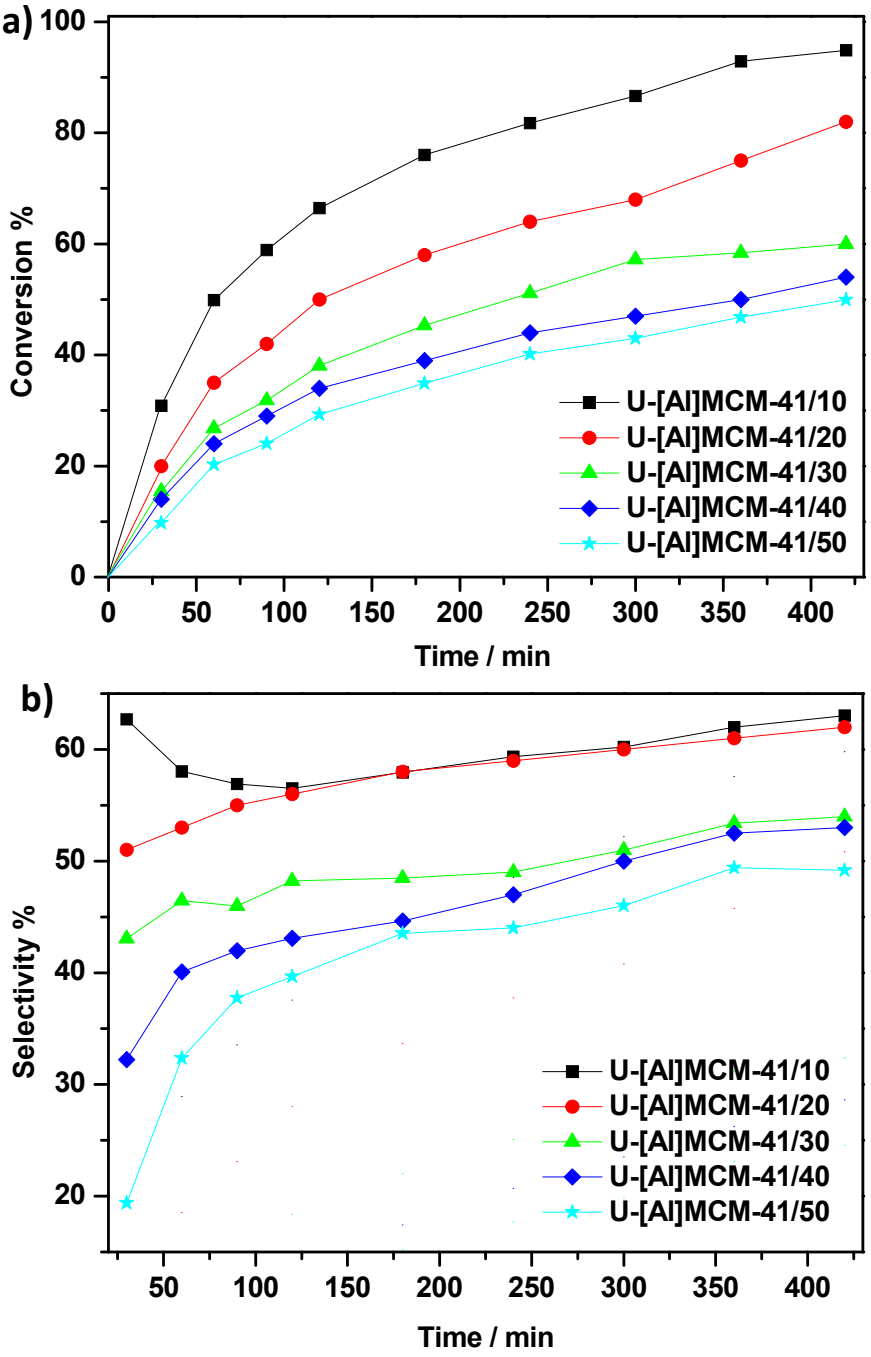
a)
Conversion %
Time / min
U-[Al]MCM-41/10
U-[Al]MCM-41/20
U-[Al]MCM-41/30
U-[Al]MCM-41/40
U-[Al]MCM-41/50
b)
Selectivity %
Time / min
U-[Al]MCM-41/10
U-[Al]MCM-41/20
U-[Al]MCM-41/30
U-[Al]MCM-41/40
U-[Al]MCM-41/50

Fig. 7

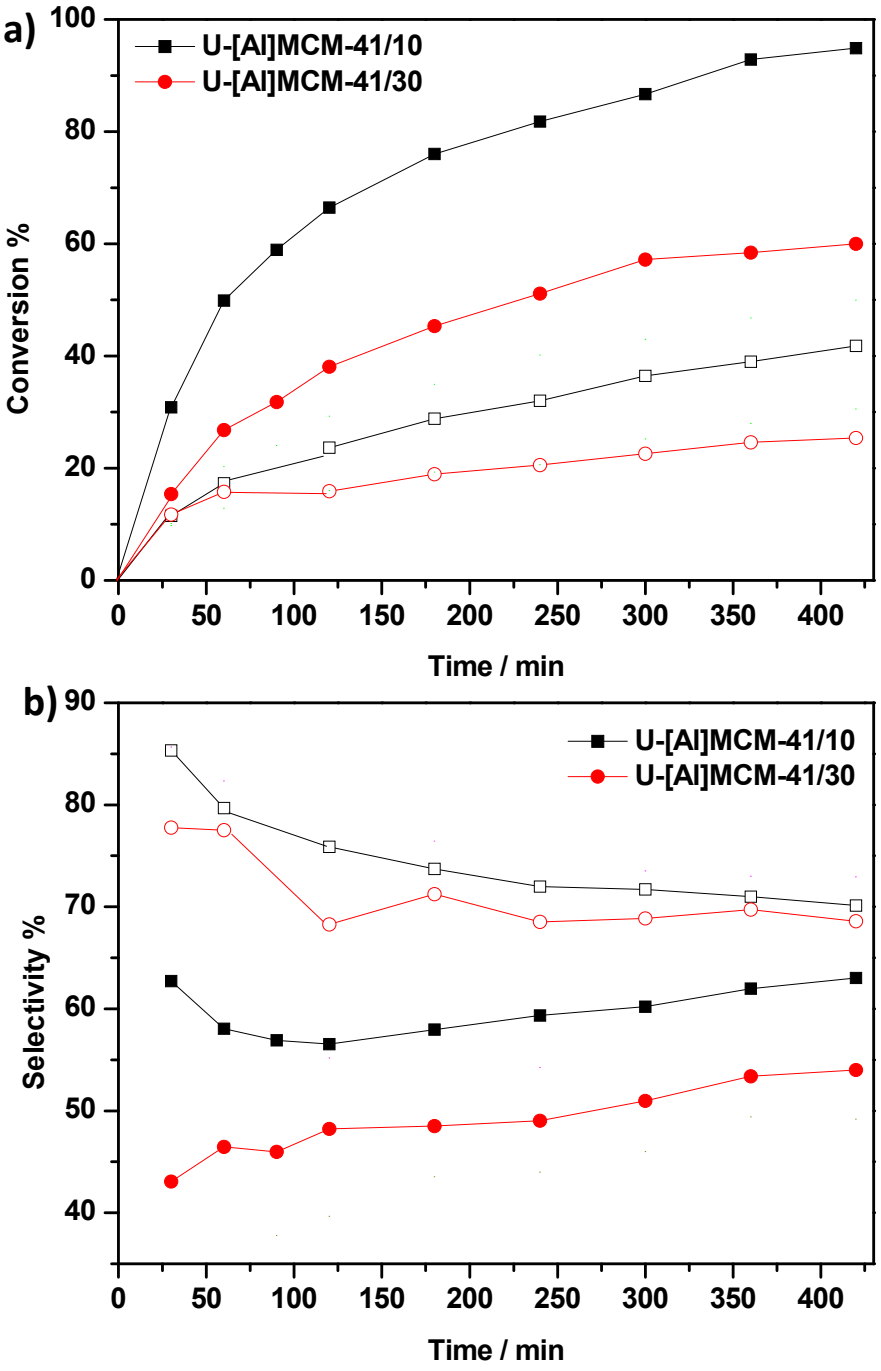
a)
U-[Al]MCM-41/10
U-[Al]MCM-41/30
Conversion %
Time / min
b)
U-[Al]MCM-41/10
U-[Al]MCM-41/30
Selectivity %
Time / min

Fig. 8

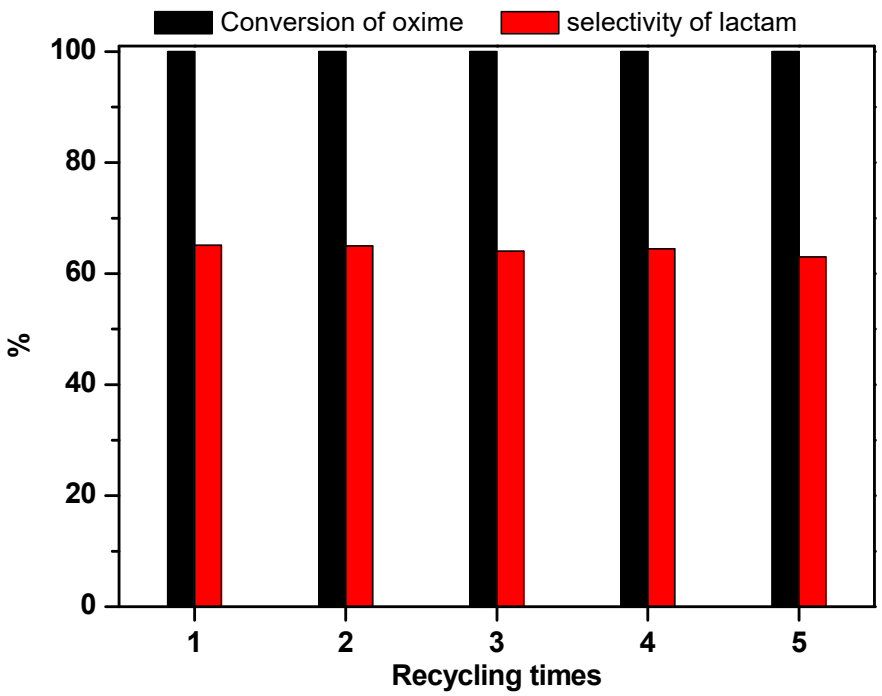
Conversion of oxime
selectivity of lactam
100
80
60
40
20
0
%
1
2
3
4
5
Recycling times

Fig. 9